Report no. 90.046

Interpretation of depth to the magnetic basement in the northern Barents Sea.

NGU
NORGES GEOLOGISKE UNDERSØKELSE

Postboks 3006 - Lade
7002 Trondheim
Tlf. (07) 92 16 11
Telefax (07) 92 16 20

RAPPORT

Rapport nr. 90.046	ISSN 0800-3416	Åpen/~~Fortrolig~~

Tittel:
Interpretation of depth to the magnetic basement in the northern Barents Sea

Forfatter: Jan Reidar Skilbrei	Oppdragsgiver: NGU, Statoil, Norsk Hydro, Norske Shell, Norsk Agip, Elf Aquitaine Norge
Fylke:	Kommune:
Kartbladnavn (M. 1:250 000)	Kartbladnr. og -navn (M. 1:50 000)
Forekomstens navn og koordinater:	Sidetall: 42 Pris: 600 Kartbilag: 2

Feltarbeid utført:	Rapportdato:	Prosjektnr.:	Seksjonssjef:
	25.05.1990	61.2440.00	Jens S. Rønning

abstract

The Geological Survey of Norway (NGU), in co-operation with Geco, conducted aeromagnetic measurements over the northern Barents Sea on behalf of the five oil companies Statoil, Norsk Hydro, Esso Norge, Elf Aquitaine Norge and Norsk Agip. The survey area, situated between 74° 30' and 77° N, and 15° and 32° E, covered some 135 000 km² with 34 000 km of aeromagnetic profiles. The study area embraces the Svalbard Platform, the Hopen High, *the Sørkapp Basin, the Bjørnøya-Sørkapp High and the continent-ocean transition* zone, as well as other major structural features. The main result of the study is a contour map of the depth to the top of the magnetic basement. The interpreted depths to the magnetic basement exceed 10 km in the Sørkapp Basin, in parts of Storfjorden, and towards the Olga Basin. The crystalline basement is found at depths of less than 2 to 3 km at the Bjørnøya-Sørkapp High and the Hopen High, and at depths of about 6 km on the Gardarbanken High. Depths in the area of the central platform vary smoothly and gradually from 6 to 9 km. It is believed that in some areas pre-Permian sediments may constitute more than half of the total sedimentary column.

The continent-ocean transition zone is clearly reflected in both the magnetic map and the magnetic basement map. Strong gradients in the contour map of depth to magnetic basement coincide with the well-known Bjørnøya-Sørkapp and the Hornsund-Fault-Zones. It is therefore believed that the strongest gradients seen elsewhere in the depth to basement map reveal major basement faults and flexures which define the margins of structural highs and deep troughs. The continental crust in the western half of the study area has been deformed in a NNW-SSE trending zone, which is parallel or sub-parallel to the trends of continuous positive magnetic anomalies observed in the same area, and sub-parallel to major tectonic lines mapped by geologists further to the north, onshore Spitsbergen. It is therefore suggested that Precambrian fault zones have been reactivated in Phanerozoic times. These basement lineaments divide the structure of the northern Barents Sea into a series of basins and highs. East of a major tectonic line running N-S to NW-SE through the central part of the area, the basement map and the aeromagnetic map show variable trends, with NE-SW trends dominating. Comparison with deep seismic reflection data suggests that the discontinuity represents a major Caledonian compressional structure (perhaps the Iapetus suture) which separates two different crustal terranes.

Emneord	Flymåling	
Geofysikk	Berggrunn	Fagrapport
Magnetometri		

LIST OF CONTENTS

ABSTRACT

The Geological Survey of Norway (NGU), in co-operation with Geco, conducted aeromagnetic measurements over the northern Barents Sea on behalf of the five oil companies Statoil, Norsk Hydro, Esso Norge, Elf Aquitaine Norge and Norsk Agip. The survey area, situated between 74^0 30' and 77^0 N, and 15^0 and 32^0 E, covered some 135 000 km^2 with 34 000 km of aeromagnetic profiles. The study area embraces the Svalbard Platform, the Hopen High, the Sørkapp Basin, the Bjørnøya-Sørkapp High and the continent-ocean transition zone, as well as other major structural features. The main result of the study is a contour map of the depth to the top of the magnetic basement. The interpreted depths to the magnetic basement exceed 10 km in the Sørkapp Basin, in parts of Storfjorden, and towards the Olga Basin. The crystalline basement is found at depths of less than 2 to 3 km at the Bjørnøya-Sørkapp High and the Hopen High, and at depths of about 6 km on the Gardarbanken High. Depths in the area of the central platform vary smoothly and gradually from 6 to 9 km. It is believed that in some areas pre-Permian sediments may constitute more than half of the total sedimentary column.

The continent-ocean transition zone is clearly reflected in both the magnetic map and the magnetic basement map. Strong gradients in the contour map of depth to magnetic basement coincide with the well-known Bjørnøya-Sørkapp and the Hornsund-Fault-Zones. It is therefore believed that the strongest gradients seen elsewhere in the depth to basement map reveal major basement faults and flexures which define the margins of structural highs and deep troughs. The continental crust in the western half of the study area has been deformed in a NNW-SSE trending zone, which is parallel or sub-parallel to the trends of continuous positive magnetic anomalies observed in the same area, and sub-parallel to major tectonic lines mapped by geologists further to the north, onshore Spitsbergen. It is therefore suggested that Precambrian fault zones have been reactivated in Phanerozoic times. These basement lineaments divide the structure of the northern Barents Sea into a series of basins and highs. East of a major tectonic line running N-S to NW-SE through the central part of the area, the basement map and the aeromagnetic map show variable trends, with NE-SW trends dominating. Comparison with deep seismic reflection data suggests that the discontinuity represents a major Caledonian compressional structure (perhaps the Iapetus suture) which separates two different crustal terranes.

INTRODUCTION

Although the northern Barents Sea is part of one of the largest epicontinental seas in the world, it is still relatively unexplored. This fact prompted the Geological Survey of Norway (NGU), in co-operation with Geco, to conduct an aeromagnetic survey for Statoil, Norsk Hydro, Norsk Agip, Elf Aquitaine Norge and Esso Norge, to identify the main structural features, to acquire information on the topography of the top of the basement, and to assist in the planning of future exploration work. The survey area lies between 15° and 32° E, and 74°30' and 78° N (see Fig. 1), and is located within the northern auroral belt. The survey was carried out during the spring and summer of 1987, and covered an area of 134 000 km^2 with profiles totalling 34 000 km in length.

Geco delivered a preliminary interpretation report of the aeromagnetic data (Myklebust, 1988). This paper will deal with the interpretation of the depth to the magnetic basement. Except for one seismic profile, the interpretation is based exclusively on the aeromagnetic data. No attempt has been made, so far, to include other kinds of geophysical data in this work. The aim of this study has been to provide information about the basement topography which is important not only in the early stages of the exploration work; the data can be reanalysed at a later stage, using additional data, to constrain the interpretation when more data types have been acquired.

The concern of a relatively large part of this study has been to compare, and gain experience with, different methods of estimating depth to magnetic sources. The basement map is the result of several manual techniques and an automatic technique applied to original profile records. In a few instances the depths have been determined from contour maps.

DATA SETS AND DATA QUALITY

Survey methods, instrumentation, and quality of aeromagnetic and positional data have been described i Skilbrei (1988), Christoffersen (1988) and Skilbrei et al. (1990).

The survey area is located inside the northern auroral zone where magnetic temporal variations are among the worst possible. Thus, the 'high-latitude magnetic problem' (diurnal variation) makes any aeromagnetic survey at these high latitudes particularly risky. Data quality is dependent primarily on the ability to acquire data during the short-lived quiet periods. Base magnetometers were set up at Bjørnøya and in Longyearbyen (see Fig. 1 for locations). In order to guarantee high quality data from the area within the budget and time allowed, the following procedure was adopted: The survey was divided into three areas (see Fig. 1) which were covered separately, in order of priority. Each area was finished (including re-flying of poor data) before the start of the next area. Profiles acquired when the magnetic time variation was stronger than 30 nT per 10 minutes (linear variation) were reflown. Data acquired when the time variation was between 15-30 nT per 10 minutes (linear) or stronger than 10 nT in 5 minutes (non-linear) were in most cases reflown. Thus, relatively good data were obtained for the area covered within the budget and limited acquisition period, instead of spending a lot of time waiting for the short-lived 'best' periods, or having data of variable quality distributed over a somewhat larger area. (A denser grid was originally planned for the western part of area III, but this was omitted for economic reasons).

The use of Global Positioning System (GPS) satellite navigation reduces errors due to mislocations, but errors due to other sources remain. Discrepancies between measurements exist at the intersection of different tracks. The flight line pattern (Fig. 1) provides some control on data quality. At every intersection two measurements of the Earth's field are made. The cross-track difference, or mistie, is the difference between a pair of such measurements. The magnitude of these mistie values will, at high latitudes, largely depend on the temporal variations in the magnetic field. The average cross-track difference (mistie) was 45.5 nT for the whole data set, before any adjustments were made. Constant corrections to each individual complete profile (zero-order levelling) brought the value down to 10.2 nT.

RESIDUAL MAGNETIC ANOMALY MAP

After diurnal and systematic line level correction, an average cross-over error at line intersections of 9,1 nT remained. To simplify gridding and contouring across the inconsistencies at the line crossings, a random error adjustment procedure was applied. The resulting random error adjusted profiles were then forced through the adjusted points by use of cubic spline functions. This procedure can severely modify anomaly shapes where inconsistencies at line crossings are significant in relation to the amplitudes and gradients of the crustal source anomalies. Therefore, the contour map cannot be used for quantitative interpretations everywhere in the map area. A simplified, residual map with a contour interval of 20 nT (shaded relief version with illumination from the east) is shown at a reduced scale in Fig. 2. A shaded relief version of a colour map, with 10 nT contour interval is shown at a reduced scale in Fig. 4, and the map is presented in the scale 1:1 mill. in Appendix 2. For this map, the gridd was generated using the minimum curvature method of Briggs (1974). A few reconnaissance profiles (12^0E-15^0E) which were flown to the west of the survey area have been included in this map as colour strips, for the sake of completeness. Trend enhancement was used in gridding data from the western provinces.

BRIEF DESCRIPTION OF THE ANOMALY MAP

Short to intermediate wavelength anomalies of moderate to high amplitudes occur to the north of Bjørnøya (Figs 2 & 4), reflecting a shallow magnetic basement. On the contour map, almost continuous positive anomalies trend NNW-SSE from this area to about 76° N. On individual east-west profiles, several anomalies can be resolved which probably reflect a magnetic basement that has been downfaulted to the west. These basement faults, are probably associated with the rifting of the continent when the Norwegian-Greenland Sea opened during the Tertiary (e.g. Eldholm et al. 1988, and references therein).

Several magnetic highs are located to the west and northwest of Bjørnøya, approximately along the 16° E line of longitude, and between latitudes 74° 30' and 76° 45' N. The bodies causing the anomalies are estimated to lie at depths between 4 and 10 km below sea level and are interpreted as Tertiary volcanic intrusions. To the south of this area, Faleide et al. (1988) interpreted a marginal high from reflection seismic data which they ascribed to Tertiary volcanism. The magnetic data suggests such Tertiary volcanism to have occurred further northeast than previously recognized.

Pronounced magnetic anomalies between 16° 30' E and 20° E trend NNW-SSE from around 76° 15' N to the margin of the survey area which is the southeastern coast of Spitsbergen. These magnetic lineaments are in line with major tectonic lineaments on Spitsbergen (see simplified geology, Fig. 1). Thus, it can be assumed that the principal basement structures on Spitsbergen must continue southwards far into the Barents Sea.

Storfjorden is characterised by narrow anomalies of weak amplitude which are probably caused by doleritic intrusions occurring just beneath the Quaternary deposits on the sea-floor. These anomalies are prominent on profiles (see Fig. 3). Due to the large flight-line spacing in this area (8km * 24 km), and the irregular nature of the anomalies, it is not possible to represent the anomalies adequately on contour maps. However, the shaded relief version of the colour map depicts the presence of high-frequency anomalies (Fig. 4 and Appendix 2). Sills and dykes are widespread throughout Barentsøya and Edgeøya (Winsnes & Worsley, 1981), especially in the western parts of the islands. Dolerites also constitute the small islands and skerries of the Tusenøyene to the south of Edgeøya. Datings of similar intrusions on Spitsbergen suggest a Late Jurassic/Early Cretaceous age for these dolerites (Winsnes & Worsley, 1981, Weigand & Testa, 1982). Analysis of the profile data does not indicate with certainty if the anomalies are caused by induced magnetization or if the dolerites are dominated by remanent magnetization. Curve-matching indicates that the anomalies are generally caused by steeply dipping magnetic bodies. It is therefore suggested that most of the anomalies are probably caused by dykes, rather than sills. The Kimmerian tectonic events, which are prominent further south, are primarily represented by intrusions and volcanism near the Jurassic-Cretaceous boundary (Steel & Worsley 1984). The intrusive activity was probably associated with extension that could have been penecontemporaneous with the Kimmerian tectonic phase. It is suggested that Storfjorden may have been the centre of the intrusive activity, where dykes predominate over sills.

The dolerite sources may obscure the response of magnetic sources that may lie at greater depths. However, the high-frequency anomalies are superimposed on a regional magnetic low (see Fig. 3). Thus, there is apparently no detectable long-wavelength anomaly originating from deeper sources.

In the eastern part of the survey area (particularly east of 27^{0} E) the anomaly picture is generally smoother than in the western areas. This is partly due to the presence of thick sedimentary basins, and also due to a basement complex which is non-magnetic to weakly magnetic (see below).

INTERPRETATION METHOD

Sedimentary formations have very weak magnetic susceptibilities in comparison with those of crystalline rocks. The main sources of magnetic anomalies are basement structures with associated magnetizations and susceptibility contrasts within the basement (e.g. Vacquier, 1972). Intrusive and extrusive igneous bodies emplaced within or over the basement give rise to magnetic anomalies. In general, the magnetic source depth corresponds to the depth to the crystalline basement.

Manual methods

In most instances the analysis has been made on original profiles using manual methods. Each anomaly that occurs on the profiles has been checked for noise, and carefully interpreted when conditions required for depth determination have been met. The interpretation has been performed on sheets displaying a vertical stack of the following profiles (in the scale 1:100,000): (1) raw total field magnetic data; (2) magnetic data after subtraction of a reference field (IGRF-1985); (3) filtered magnetic data; (4) calculated 1. vertical derivative of the magnetic profile; (5) base magnetic data from both Bjørnøya and Longyearbyen; and (6) radar altimetry. A redrawn version of a vertical stack is shown at a reduced scale in Fig. 3 (profile no. BSA-7714-3-A, crossing Storfjorden from west to east). From such a display it is easy to distinguish anomalies caused by crustal sources from those that could be due to magnetic time variations. Of course, the assumption is made that no magnetic disturbances occurred in the acquisition area without also occurring at one of the two base stations. Such an assumption can be wrong when interpreting data from the eastern area because the distance from the two base monitors to 32^0 is equal to c. 1/20 of the Earth's circumference at these latitudes.

A review of the various methods of manual interpretation of magnetic data by the use of characteristic points and distances in the anomaly curves was published by Åm (1972). These are the straight slope method, Sokolov's length and Peter's length. It is important to realise that these methods are valid only when certain geological conditions are fulfilled. For example, the half-slope method of Peter was derived for magnetic anomalies over vertical dykes of infinite strike length with vertical magnetic polarization (Peters, 1949). To obtain the correct depth, the depth estimator used must in each case be divided by a certain factor which is dependent on the form and the dimension of the causative body, which has been estimated by the aid of suitable interpretation chart given in Åm (1972).

The interpretation has been made using characteristic points and distances in the anomaly curves. All the three above-mentioned methods have been used where possible. The results have been compared with the depths obtained from an automatic method (the autocorrelation method, see below). For each anomaly, either the estimated depth thought to be most reliable has been used, or the average of two to four different estimates resulting from the use of different methods. In the easternmost areas, where the original records are curvilinear, it was difficult to use the Peters length and the straight slope length. However, the Sokolov length, when averaged from two neighbouring profiles flown in opposite directions, gave results close to those obtained on redrawn profiles and those obtained by the method of Vacquier et al. (1951). Even so, there are large areas in the eastern part of the survey area which show no well defined anomalies to yield reliable basement depths.

The method of Vacquier et al. (1951) has been used as an additional method for two reasons. First, it takes into account the dimensional geometries of vertical prisms having different orientations with respect to the magnetic north. Vacquier et al. (1951) computed a large number of model anomalies for rectangular prisms, and gave correction factors to be multiplied with the straight-slope length, which is measured on different flanks of the anomaly on a contour map, in order to obtain the depth to the causative body. Secondly, where a magnetic profile shows no well-defined straight-slope lengths it was tested to see if the straight-slope length measured on contour maps could be used.

In this study it was found that the analysis made on the profile data gave the most reliable results. This is perhaps to be expected for the following reasons. First, the process of contouring the data set inevitably involves, to some degree, a smoothing of the original data. Secondly, both the flight lines (flown east-west) and tie-lines (flown perpendicular to the east-west lines) have been used in the gridding. This means that the discrepancies at line crossings, which are left after systematic flight line corrections, have to be distributed along lines in a nearly random way before the grid can be generated from the data. Therefore, the actual form of the anomaly will, in some locations, be distorted. Thirdly, when interpreting the profile lines, only the data free of diurnal noise have been used, whereas the contour map contains some diurnal noise since the process of contouring uses all 'accepted' data (data which are kept after re-flying of poor data; see Skilbrei et al., 1990). The distortion of anomalies on the contour map is most severe in areas showing a weak horizontal gradient.

The autocorrelation method.

The analysis uses the autocorrelation algorithm developed by

Phillips (1975, 1978), which utilizes the maximum entropy method of Burg (1967, 1968, 1975). Magnetic source depth values are estimated from the autocorrelation coefficients of short samples of magnetic profile data. This method gives four depth estimates at each point along a magnetic profile. The estimated depth values are calculated in a computationally efficient manner and inaccurate estimates are easily discarded on the basis of their relative lack of convergence.

When using the autocorrelation analysis algorithm (Phillips, 1975, 1978), one has to assume that the sources are dykes of semi-infinite extent lying approximately perpendicular to the track, and that the magnetization function along the track can be presented as an uncorrelated white noise sequence. Autocorrelation coefficients are calculated for a series of short data sets abstracted from the data are calculated; then, the well-known relationship between the source depth and the autocorrelation function of a magnetic profile (see, for example, Serson & Hannaford, 1957) is used to calculate the source depth. A complete description of the method can be found in Phillips (1975). Appendix 1 presents a brief description of the method. The applied version of the computer programme has been provided by Thorning (1982) at the Geological Survey of Greenland.

ERROR ANALYSIS

The accuracy of the interpretation map (Fig. 5 & App. 3) is difficult to estimate. The author is ready to admit the standard 10-15% error on individual depth determinations as quoted in the literature (Vacquier et al. 1951, Steenland 1963). It is the author's experience (Skilbrei 1989a) that this error applies to the precision of the estimate itself. The systematic errors associated with situations where the assumptions that the method require are not fulfilled, for example, a neglected bottom effect, can lead to large errors (Åm 1972, Skilbrei 1989a). Åm (1972) estimated the error to be around 30% when the magnetic source structure is 3-Dimensional. Skilbrei (1989a) has shown that when the vertical depth extent (h=distance from top to bottom) of the body is equal to the depth (d) to the top of the body, the depth will be underestimated by a factor whose magnitude is dependent on the ratio of the width (w) of the body to the depth (d) to the top surface. On the other hand, Steenland (1970) believed that if the vertical depth extent is equal to or greater than that of the depth to the top (d), the depth extent, for practical purposes, may be regarded as infinite. Henderson (1966), found that, on the basis of model studies, the ratio of the vertical depth extent (h) to the depth (d) has to be 8 or greater before the depth extent can be regarded as infinite.

It is important to realise that the errors will show geographical variation since poorly defined anomalies, or anomalies disturbed by neighbouring anomalies, or the presence of noise in the data, yield uncertain results. The fallibility of the magnetic method was clearly demonstrated by Jacobsen (1961). However, if the method is used in conjunction with other geophysical data, the results are useful and reliable (Jacobsen 1961, Steenland 1963, Åm 1972). The author recommends that the data be compared with reflection data (if available) in areas where anomalies are poorly defined or where only a few anomalies are present. However, correlation between magnetic basement and acoustic basement may not always be expected (see discussion below).

The top of the magnetic basement may not always coincide with the 'true' basement. Intrusions may be present within the sedimentary column. In most cases this can be discerned from the data, due to a shorter wavelength content in the aeromagnetic data. The magnetic sources within the basement may not reach the top of the basement. In this area, the following geological reasons for such a situation to exist seem plausible: (1) Rocks of Early Paleozoic age (Hecla Hoek successions), dominate in the western and northern part of Spitsbergen (see e.g. Birkenmajer 1981, Ohta et al. 1983). The Hecla Hoek is commonly non-magnetic and can be situated upon Precambrian basement rocks which are magnetic. Thus, it cannot be ruled out that 'sheets' of Hecla Hoek rocks may overlie the

Precambrian basement. However, Hecla Hoek rocks exposed in Svalbard are steeply dipping (which means that the lithological variations produce 'intrabasement type anomalies'). (2) Granulite-facies rocks normally show higher magnetization than lower grade rocks (Powell 1970, Larsen, C.L. 1980, Schlinger 1983, 1985, 1989, Grant 1985, Olesen et al. 1990, Skilbrei et al. 1990). Quite commonly, high-grade metamorphic rocks may occur beneath basement rocks of lower grade. Fortunately, highly deformed basement complexes most often show steeply dipping foliation and contacts which contribute to producing magnetic anomalies caused by intrabasement susceptibility contrasts where the top of the magnetic basement is the 'true' top of the basement. (3) Non-magnetic Late Precambrian (Vendian) or Early Palaeozoic metasedimentary rocks overlie Precambrian basement in Finnmark (Sigmond et al. 1983), on Bjørnøya (Worsley & Edwards 1976) and probably also in the southern Barents Sea (Åm 1975a, 1975b). Such a situation may also occur in the northern Barents Sea. In addition, it must be mentioned that the Devonian 'Old Red Sandstone' exposed on Spitsbergen is non-magnetic (Kurinin 1965) with densities close to that of basement rocks with acidic to intermediate composition. Devonian basins may occur beneath post-Devonian basins on Spitsbergen and in the northern Barents Sea. Due to their comparatively high density, and thus high seismic velocities, the Devonian rocks may be misinterpreted as forming the top of the crystalline basement in the seismic reflection data. (4) Inhomogeneous susceptibility variation within a magnetic body yields too shallow depth estimates (Bystøl 1988). Bystøl (1988) calculated the anomalies above vertical thick dykes which were composed of a central part with the largest susceptibility values, and with the susceptibility decreasing linearly outwards in both directions (perpendicular to the strike of the dyke) from the centre of the dyke. The magnitude of the underestimation increases with increasing values of the ratio w/d.

CONTOUR MAP OF THE TOP OF THE MAGNETIC BASEMENT

Depths have been determined for all magnetic anomalies (which do not correlate in time of acquisition with the occurrence of diurnal noise at the two base magnetometer readings) in the area. Corrections for anomaly strike have been made. After a critical examination of the results, a generalised contouring of the basement surface was made. Less weight has been given to uncertain determinations and to values which differ too much from the others.

Fig. 5 and Appendix 3 show a generalised contour map of the magnetic basement surface. The location of each individual depth estimate is shown by a dot on the map.

Structure of the basement

Major faults in the basement have been identified by sharp gradients in the magnetic basement depths, and marked on the interpretation map together with possible/uncertain faults (Fig. 5 and App. 3). The interpretation of faults is considered to be conservative. Outside the Svalbard platform, the faulted basement produces a relief of structural highs and deeps. In the central part of the area, three major basement highs appear which are identified as the Bjørnøya-Sørkapp High (also named Stappen High), Hopen High and Gardarbanken High. This clearly demonstrates that the basement map shows features which correlate with the known structure of the basins and highs. Just to the west of the Bjørnøya-Sørkapp High is a steeply dipping NNW-SSE trending fault which, in position, can be related to the Bjørnøya-Sørkapp Fault Zone that continues to the northwest west of Spitsbergen. Further to the west of the Bjørnøya-Sørkapp High, the basement depth increases rapidly. The magnetic basement remains deep further towards the 17^0 E line of longitude. Myhre & Eldholm (1987) proposed that the Hornsund Fault Zone forms a hinge line for the post-opening marginal subsidence. The deep basement in this area underlies the Cenozoic sedimentary wedge which covers the entire margin of the area (Faleide & Gudlaugsson 1981, Faleide et al. 1984a, Faleide et al. 1988, Spencer et al. 1984, Eldholm et al. 1987, Riis & Vollset 1988). West of approximately 17^0 E the magnetic basement becomes shallower and the magnetic map acquires N-S and NNE-SSW magnetic trends. These trends are probably associated with volcanic and subvolcanic rocks extruded and intruded during rifting of the lithosphere. The rifting occurred in the Early Tertiary when the Norwegian-Greenland Sea started to open (Eldholm et. al 1988). Thus, the transition zone between continental and oceanic crust has been interpreted from the magnetic data to lie between these anomalies and the magnetic flat region towards Bjørnøya (Fig. 4). The proposed transition zone is marked on the map (Fig. 5 and App. 3). It is situated 10-15 km further to the east than the location proposed by Eldholm et al. (1987).

There are maximum thicknesses of sediments exceeding 10 km in the Sørkapp Basin, in the southern part of Storfjorden, and towards the Olga Basin in the extreme east.

Structural trends

Magnetic rocks are exposed on the western part of Sørkapp (Åm 1975a, Skilbrei et al. 1988). South and east of Sørkapp, the depths to the magnetic sources increases rapidly. The Central Basin on Spitsbergen (see simplified geology in Fig. 1) continues southwards into the northern Barents Sea, to about 76^0 15' N. This seaward extension of the Central Basin is also probably outlined by the gravity low discernible on the gravity map which covers the area (Faleide et al. 1984b). The aeromagnetic map (Figs 2 & 4) and the basement map (Fig. 5 and App. 3) in this region show a distinctive NNW-SSE trend, which is the trend of the Hecla Hoek rocks and of the main tectonic boundaries on Svalbard (see Fig. 1, Harland 1965, 1966, 1969, 1975, Hjelle et al. 1979, Hjelle & Lauritzen 1982, Ohta 1982). As seen from the aeromagnetic map (Figs 2 & 4) and the basement map (Fig. 5 and App. 3), the western half of the project area shows NNW-SSE structural trends, while the eastern area is more variable with NNE-SSW structural trends predominating.

Rocks of Late Proterozoic to Early Palaeozoic age (the Hecla Hoek) dominates in the northern and western parts of Svalbard (Fig. 1, Birkenmajer 1981, Ohta et al. 1983). During this period the NNW-SSE structural lineaments, which were probably reactivated by subsequent tectonic events, were established (Harland et al. 1974, Birkenmajer 1981, Mann & Townsend 1989). The Late Devonian Svalbardian tectonic phase affected the Old Red Devonian basins and sinistral strike-slip motion took place along the older lineaments (Birkenmajer 1975). A more stable period characterized Carboniferious and Early Permian times, and the area became a stable platform in the Late Permian (Birkenmajer 1981).

The whole area between Bjørnøya, Sør-Kapp, Storfjorden and the Sør-Kapp basin is characterised by NNW-SSE trending anomalies that are uniform over long distances. These uniform anomalies support the idea of large-scale displacement along NNW-SSE trending basement faults or zones of weakness which probably reflect an original Caledonian trend. This trend is, in turn, probably inherited from a pre-Caledonian trend, as is the case with many structural trends on Svalbard (see refs. given above). It is therefore suggested that Precambrian structural trends have pre-determined lines of weakness in Phanerozoic times. Such distinct magnetic lineaments can be linked to the tectonic trends on Svalbard. Thus, the tectonic framework in the basement on Spitsbergen, and over a large part of the adjacent northern Barents Sea, is essentially similar. This is not a new idea since Harland (1969, 1975, 1980), Harland & Gayer (1972) and Harland et al. (1974) have proposed similar interpretations. The work reported here, however, is the first documented study of data which cover large areas of the northern Barents Sea; and more important, the magnetic data can be regarded as a direct expression of the structure of the basement and the lithological structures within the basement.

As mentioned above, the NNW-SSE and N-S trends are known to be present on the Svalbard archipelago (e.g. Harland 1974) where there is compelling evidence that reactivation of Precambrian fracture zones has taken place in Phanerozoic times. In contrast, east of about 20^0E line of longitude, structural trends are, generally, NE-SW oriented. If the same genetic links exist between the (NE-SW) trends seen today in this area and the Caledonian and Precambrian trends in the basement, as there is evidence of in the western half of the survey area, then the aeromagnetics delineate a NNW-SSE oriented tectonic zone (the interpreted tectonic zone is marked on Fig. 5 and App. 3) which separates structurally markedly different continental terranes (see discussion below).

That this zone is real and that it must be of pre-Mesozoic origin is supported by a deep seismic reflection line running NNW-SSE across the Svalbard platform (see Fig. 6 for the profile, and Fig. 1 for location of profile). According to Gudlaugsson et al. (1987), a zone of thrust-faulting separates highly reflective crust in the west from a province of lesser reflectivity in the east. As seen from Fig. 6, a band of westward dipping reflections seems to define a continuous feature. The asymmetric nature of the reflection pattern could be consistent with eastward directed overthrusting. Gudlaugsson et al. (1987) have suggested this feature to represent the main suture zone resulting from the closure of the Iapetus ocean. I should like to point out that the reflection line represents only one profile, and that variations in reflection patterns are likely to occur along the interpreted tectonic line. The geology of Svalbard indicates the 'Caledonian' rocks (Hecla-Hoek) there can be correlated with Caledonian rocks in East Greenland (Hambrey 1989, Herrington & Fairchild 1989). Extrapolating the tectonic feature observed on the seismic records along the zone which separates two different areas showing approximately perpendicular structural trends (magnetic trends thought to represent basement features) would bring the zone onto Spitsbergen between 17^0 E and 18^0 E, which is close to the southern extensions of the Billefjorden Fault Zone and the Lomfjorden fault. These interpretations emphasize the importance, and the long-lived nature, of these faults.

DISCUSSION OF RESULTS

The depth to the magnetic basement map (Fig. 5 and Appendix 3) is believed to present a fairly accurate, albeit generalised and smoothed picture of the depth to the top of the magnetic basement in the area. It is thought to be most accurate in the western half of the area, where well defined anomalies occur which provide reliable basement depths. In the east, where the basement is less magnetic, the depth estimates are uncertain. However, the anomalies are weak in amplitude, partly because their causative bodies lie at great depths. The basement map in this area also shows features that correlate with known structural features; such as the Sentralbanken High, the Gardarbanken High, and basins known as the Olga Basin (which extends from the northeastern margin of the survey area to east of the 32^{0}E line of longitude), and the Sørkapp basin. (Thus, it is not an overinterpretation to present a map which shows a generally deep magnetic basement in this eastern area).

The basement map will, in most cases, represent the top of the crystalline continental crust in the area, and of the thickness of the non-magnetic rocks, i.e. the sedimentary cover overlying this crust (after the known water depth has been removed). It is important to realise that the magnetic basement map generally corresponds to the Precambrian basement. Hecla Hoek rocks, and the Old Red Sandstone (Devonian) are generally non-magnetic with associated high densities (Kurinin 1965), which make these successions a part of the acoustic basement. With the exception of suprabasement magnetic rocks, and negative errors in the depth estimates (underestimated depths) associated with 3-D structures (see App. 1), the depth to magnetic source analysis yields maximum basement depths, since magnetic sources may be situated below non-magnetic crystalline rocks.

The main structures in the study area have been identified. It is obvious from Fig. 5 that in the west, the dominant structural features is a NNW-SSE trending basement high area (from Bjørnøya towards Sørkapp). To the west, this zone is limited by the Bjørnøya-Sørkapp Fault. Further west, there is a deep sedimentary basin, limited by the Hornsund Fault Zone in the west which is close to the continental-oceanic crust boundary. West of the Hornsund Fault Zone the trends are more variable, with NE-SW and NNW-SSE strike trends dominating. (These trends are associated with rift and shear structures created during the initial rifting of the lithosphere associated with the opening of the Norwegian-Greenland Sea).

While dolerite intrusions are widespread in Storfjorden, and may obscure the magnetic response originating from the crystalline basement below Storfjorden, the northern Barents Sea is generally devoid of magnetic anomalies which could be caused by intrasedimentary intrusions. Therefore, the basement map presented here provides information on the topography of the top of the basement in an area where geophysical and geological information is sparse.

The southern part of Storfjorden shows a basement surface lying at great depths (> 10 km). The magnetic trends in Storfjorden indicate roughly N-S trends. It is possible that a basin continues to the north along the centre of Storfjorden, between 18^0 30' E and 20^0 30' E. This basin is, at least in the west, interpreted to be fault bounded. If this interpretation is correct, then a large basement fault exists in the Storfjorden.

The basement map (Fig. 5) shows trends which are related to the structural highs and lows. In addition, the aeromagnetic map (Figs 2 & 4) shows trends that also reflect structures within the Precambrian and/or Caledonian basement. There is a clear NNW-SSE trend and a N-S trend between 17^0 E and 22^0 E, and evidence of a NE-SW trend in the eastern half of the survey area (particularly in the Hopen High area and along the southeastern margin of the survey area). On Svalbard, there is compelling evidence of long-lived basement fault zones (e.g. Andresen at al. 1986, Mann & Townsend 1989). It is thought that many of the magnetic trends are expressions of rejuvenated older zones of weakness present in the basement, some of which divide the structure of the basement over large ares of the study areas into a series of basins and highs (Fig. 5).

SUMMARY

The main result of the study is a contour map of the depth to the top of the magnetic basement. There are maximum thicknesses of sediments exceeding 10 km in the Sørkapp Basin, in the southern part of Storfjorden, and towards the Olga Basin in the extreme east of the survey area. The crystalline basement is found at depths of less than 2 to 3 km on the Bjørnøya-Sørkapp High and the Hopen High, and at depths of about 6 km on the Gardarbanken High. The depths on the central platform area vary smoothly from 6 to 9 km. It is believed that in some areas pre-Permian sediments may constitute more than half of the total sedimentary column.

The continent-ocean transition zone is clearly reflected in both the magnetic map and the basement map. Strong gradients in the contour map of depth to the magnetic basement coincide with the well-known Bjørnøya-Sørkapp Fault Zone, and the Hornsund Fault Zone. It is therefore believed that the strongest gradients seen elsewhere in the depth to basement map reveal major basement faults and flexures which define the margins of structural highs and deep troughs. The continental crust in the western half of the study area has been deformed in a NNW-SSE trending zone, which is parallel or sub-parallel to the trends of continuous positive magnetic anomalies observed in the same area, and sub-parallel to major tectonic lineaments mapped by geologists further to the north, onshore Spitsbergen. It is therefore suggested that Precambrian fault zones have been reactivated in Phanerozoic times. These basement lineaments divide the structure of the northern Barents Sea into a series of basins and highs.

East of a major tectonic line running in a N-S to NW-SE through the central part of the area, the basement map and the aeromagnetic map show variable trends, with NE-SW trends dominating. Comparison with deep seismic reflection data suggests that the discontinuity represents a major Caledonian compressional structure, (perhaps the Iapetus suture) which separates two different crustal terranes.

ACKNOWLEDGEMENTS

We thank Statoil a.s, Elf Aquitaine Norge a.s., Norsk Hydro a.s., Norsk Agip a.s. and Esso Norge a.s. for financial support and their active interest during the survey. A particular word of thanks goes to the crew of the aircraft. Dr. D. Roberts, NGU, corrected the English text.

REFERENCES

Andresen, A., Strand, K., Dypvik, H., Nagy, J., Eikeland, T.A., Haremo, P. & Nesteby, H. 1986: Mesozoisk kontra Tertiær tektonisk aktivitet langs Billefjord-lineamentet syd for Isfjorden, Spitsbergen. Abstract, Norsk Geol. Foren. X. Landsmøte, Trondheim 1987. Geolognytt 21, p.14.

Andresen, A., Haremo, P. & Bergh, S.G. 1988: The southern termination of the Lomfjorden Fault Zone; evidence for Tertiary compression on east Spitsbergen. Norsk Polarinstitutt, Rapport 46, 75-78.

Birkenmajer, K. 1975: Caledonides of Svalbard and plate tectonics. Bull. Geol. Soc. Denmark 24, 1-19.

Birkenmajer, K. 1981: The Geology of Svalbard, the western part of the Barents Sea, and the continental margin of Scandinavia, In: The Ocean Basins and Margins (Eds. A.E.M. Nairn, M. Churkin, Jr. and F.G. Stehli), Vol. 5, The Arctic Ocean, 265-329.

Briggs, I.C. 1974: Machine contouring using minimum curvature. Geophysics 39, 39-48.

Burg, J.P. 1967: Maximum entropy spectral analysis, paper presented at the 37th meeting, Soc. Explor. Geoph., Onklahoma City, Onkl.

Burg, J.P. 1968: A new analysis technique for time series data, paper presented at the NATO Advanced Study Institute of Signal Processing, Enschede, Netherlands.

Burg, J.P. 1975: Maximum Entropy Spectral Analysis. Ph.D. Thesis, Stanford Univ., 123 pp., University Microfilms Int'l, Michigan.

Bystøl, L. 1988: Dybdeestimering og inhomogen susceptibilitet. En teoretisk undersøkelse av dybdeestimering til tykke plater med en lineært varierende symmetrisk susceptibilitet. Can. real. Thesis (in Norwegian), University of Bergen. 158 pp.

Christoffersen, T. 1988: Confidential Processing report BSA-87 (Barents Sea Aeromagnetic Survey, 1987). Geco, Kjørbokollen, Oslo, 41 pp.

Eldholm, O., Faleide, J.I. & Myhre, A.M. 1987: Continent-ocean transition at the western Barents Sea/Svalbard continental margin. Geology 15, 1118-1122.

Eldholm, O., Myhre, A.M., Faleide, J.I., Gudlaugsson, S.T. & Skogseid, J. 1988: Structure and evolution of passive continental margins and adjacent areas: research within the framework of the International Lithosphere Program

1985-1987. Nor. Geol. Unders. Special Publ.,3, 29-38.

Faleide, J.I. & Gudlaugsson, S.T. 1981: Geology of the western Barents Sea - A regional study based on marine geophysical data, Cand. real. thesis, University of Oslo. 160 pp.

Faleide, J.I., Gudlaugsson, S.T. & Jacquart, G. 1984a: Evolution of the western Barents Sea. Marine Petrol. Geol. 1, 123-150.

Faleide, J.I., Gudlaugsson, S.T., Johansen, B., Myhre, A.M. & Eldholm, O. 1984b: Free-air gravity anomaly maps of the Greenland Sea and the Barents Sea, Norsk Polarinstitutt Skrifter 180, 63-67.

Faleide, J.I., Myhre, A.M. & Eldholm, O. 1988: Early Tertiary volcanism at the western Barents Sea margin. In: Morton, A.C. & Parson, L.M. (eds.), 1988, Early Tertiary Volcanism and the Opening of the NE Atlantic, Geological Society Special Publication No. 39, 135-146.

Flood B., Nagy, J. & Winsnes, T.S. 1971: Geological map of Svalbard 1:500 000. Sheet 1G, Spitsbergen, Southern Part. Norsk Polarinstitutt Skrifter 154 A, Map and Explanatory Notes.

Gjelsvik, T. 1979: The Hecla Hoek ridge of the Devonian Graben between Liefdefjorden and Holtedahlfonna, Spitsbergen. Norsk Polarinstitutt Skrifter, 167, 63-71.

Grant, F.C. 1985: Aeromagnetics, geology and ore environments, I. Magnetite in igneous, sedimentary and metamorphic rocks: an overview. Geoexploration, 23, 303-333.

Gudlaugsson, S.T., Faleide, J.I., Fanavoll, S. & Johansen, B. 1987: Deep seismic reflection profiles across the western Barents Sea. Geophys. J. Roy. Astr. Soc. 89, 273-278.

Hambrey, M.J. 1989: The Late Proterozoic sedimentary record of east Greenland: its place in understanding the evolution of the Caledonide Orogen. In: The Caledonide Geology of Scandinavia (ed: R.A. Gayer), Graham & Trotman 1989, 257-262.

Haremo, P. & Andresen, A. 1988: Tertiary movements along the Billefjorden Fault Zone and its relation to the West-Spitsbergen Orogenic belt. Norsk Polarinstitutt Rapport, 46, 71-74.

Harland, W.B. 1965: The tectonic evolution of the Arctic-north Atlantic region. Royal Soc. London Philos. Trans. 258, 59-75.

Harland, W.B. 1966: A hypothesis of continental drift tested against the history of Greenland and Spitsbergen.

Cambridge Res. 2, 18-22.

Harland, W.B. 1969: Contribution of Spitsbergen to understanding of tectonic evolution of the North Atlantic Region. In: Kay, M. (ed) North Atlantic Geology and Continental Drift. Memoir of the American Association of Petroleum Geologists, 12, 817-851.

Harland, W.B. & Gayer, R.A. 1972: The Arctic Caledonides and earlier oceans. Geol. Mag. 109, 289-304.

Harland, W.B., Cutbill, J.L., Friend, P.F., Gobbett, D.J., Holliday, D.W., Maton, P.I., Parker, J.R., & Wallis, R.H. 1974: The Billefjorden Fault Zone, Spitsbergen - the long history of a major tectonic lineament. Norsk Polarinstitutt Skrifter, 161, 72 pp.

Harland, W.B. (1975): Paleogene correlation in and around Svalbard. Geol. Mag. 112, 421-429.

Harland, W.B. 1980: Comments on 'A palaeomagnetic pole position from the folded Upper Devonian red beds, and its tectonic implications'. Geology 8, 258-9.

Henderson, R.G. 1966: Field continuation and the step model in aeromagnetic interpretation. Geophysical Prospecting, 14, 4, 528-546.

Herrington, P.M. & Fairchild, I.J. 1989: Carbonate shelf and slope facies evolution prior to Vendian glaciation, central East Greenland. In: The Geology of Scandinavia (ed: R.A. Gayer), Graham & Trotman 1989, 263-273.

Hinz, K. & Schluter, H.U. 1978: The geological structure of the western Barents Sea. Marine Geol. 26, 199-230.

Hjelle, A. & Lauritzen, 1982: Geological map of Svalbard 1:500,000. Sheet 3G. Spitsbergen Northern Part. Norsk Polarinstitutt Skrifter, 154 E.

Hjelle, A., Ohta, Y., & Winsnes, T.S. 1979: Hecla Hoek rocks of Oscar II Land and Prins Karl Forland, Svalbard. Norsk Polarinstitutt Skrifter, 167, 145-169.

Jacobsen, P. 1961: An evaluation of basement depth determinations from airborne magnetometer data. Geophysics 24, 309-319.

Kovacs, L.C. & Vogt, P.R. 1982: Depth-to-magnetic source analysis of the Arctic Ocean region. Tectonophysics 89, 255-294.

Kurinin, R.G. 1965: Density and magnetic susceptibility of Spitsbergen rocks. In: V.N. Sokolov (Ed.): Materiala po geologii Spitsbergena. Ins. for Geology of the Arctic. Leningrad., 276-284. Translated into English 1970. National lending Libr. Yorkshire, England.

Lamar, D.L., Reed, W.E. and Douglass, D.N. 1986: Billefjorden Fault Zone, Spitsbergen: Is it part of a major Late Devonian Transform? Geological. Soc. of America Bull., 97, 1083-1088.

Larsen B. T., 1988. Tertiary thrust tectonics in the east of Spitsbergen, and implications for the plate-tectonic development of North Atlantic. Norsk Polarinstitutt Rapport, 46, 85-88.

Larsen, H.C. 1981: A high-pressure granulite facies complex in north-west Payers Land, East Greenland fold belt. Bull. geol. Soc. Denmark, 29, 161-174.

Lowell, J.D. 1972: Spitsbergen Tertiary orogenic belt and the Spitsbergen Fracture Zone. Geol. Soc. Am. Bull. 83, 3091-3102.

Mann, A. & Townsend, C. 1989: The post-Devonian tectonic evolution of southern Spitsbergen illustrated by structural cross-sections through Bellsund and Hornsund. Geol. Mag. 126 (5), 549-566.

Myhre, A.M., Eldholm, O. & Sundvor, E. 1982: The margin between Senja and Spitsbergen fracture zones: implication from plate tectonics. Tectonophysics 89, 33-50.

Myhre, A.M. & Eldholm, O. 1988: The western Svalbard margin (74^0-78^0 N). Marine and Petroleum Geology 5, 135-156.

Myklebust, R. 1988: Preliminary interpretation report: BSA-87 (Barents Sea Aeromagnetic Survey, 1987). Confidential report. Geco a.s., Kjørbokollen, Oslo. 70 pp.

Nettleton, L. L. 1971: Elementary gravity for geologist and seismologists. SEG-Monograph 1, 121pp.

Nøttvedt, A., Livbjerg, F. & Midtbø, P. S. 1988: Tertiary deformation of Svalbard - various models and recent advances. Norsk Polarinstitutt Rapport No. 46, 79-84.

Ohta, Y. 1982: Caledonian Fractures on Svalbard. In: Proceedings of the Fourth International Conference on Basement Tectonics. Eds: Gabrielsen, R. H., Ramberg, I.B., Roberts, D., Steinlein, O.A. Inter. Basem. Tect. Assoc. Publ. no. 4, 24-31.

Ohta, Y. et al. 1983: Additional evidence of pre-Silurian high-pressure metamorphic rocks in Spitsbergen. Polar Research, 2, 215-218.

Olesen, O., Roberts, D., Henkel, H., Lile, O.B. & Torsvik, T.H. 1990: Aeromagnetic and gravimetric interpretation of regional structural features in the Caledonides of West Finnmark and North Troms, Northern Norway. Nor. geol. unders. Bull. 314 (in press).

Olesen, O., Henkel, H., Kaada, K. & Tveten, E. 1990: Petrophysical properties of a prograde amphibolite - granulite facies transition zone at Sigerfjord, Vesterålen, Northern Norway, Tectonophysics (in press).

Peters, J.L. 1949: The direct approach to magnetic interpretation and its practical application. Geophysics, 14, 290-320.

Phillips, J.D. 1975: Statistical analysis of magnetic profiles and geomagnetic reversal sequences. Ph.D. thesis. Stanford University, 134 pp.

Phillips, J.D. 1978: ADEPT: a program to estimate depth to magnetic basement from sampled magnetic profiles. U.S. geol. Surv. Comput. Contr., 35 pp.

Phillips, J.D. 1979: ADEPT: A program to estimate depth to magnetic basement from sampled magnetic profiles. U.S. geol. Surv. open-file report, 79-367.

Powell, D.W. 1970: Magnetized rocks within the Lewisian of Western Scotland and the Southern uplands. Scott. J. geol. 6, 353-369.

Ram Babu, H.V., Vijayakumar, V. & Atchuta Rao, D. 1986: A simple method for the analysis of magnetic anomalies over dike-like bodies. Geophysics, 51, 1119-1126.

Riis, F. & Vollset, J. 1988: A preliminary interpretation of the Hornsund Fault Complex between Sørkapp and Bjørnøya. Norsk Polarinstitutt Rapport no. 46, 91-92.

Ringset, N. & Andresen, A. 1988: The Gipshuken Fault System-evidence for Tertiary thrusting along the Billefjorden Fault Zone. Norsk Polarinstitutt Rapport, 46, 67-70.

Schlinger, C. M. 1983: The magnetic petrology of the deep crust and the interpretation of regional magnetic anomalies. Unpubl. Ph.D. thesis, John Hopkins Univ., Baltimore, 241 pp.

Schlinger, C. M. 1985: Magnetization of lower crust and interpretation of regional magnetic anomalies: Example from Lofoten and Vesterålen, Norway. J. Geophys. Res. 90, 11484-11504.

Schlinger, C.M. 1889: Magnetism and Transmission Electron Microscopy of Fe-Ti Oxides and Pyroxenes in a Granulite From Lofoten, Norway. Journ. of Geoph. Res., Vol. 94, No. B10, 14,009-14,026.

Schluter, H.U. & Hinz, K. 1978: The continental margin of west Spitsbergen. Polarforschung 48, 151-169.

Serson, P. H. and Hannaford, W.L.W. 1957: A statistical analysis of magnetic profiles. J. Geoph. Res., 62, 1-18.

Sigmond, E.M.O., Gustavsson, M. & Roberts, D. 1984: Berggrunnskart over Norge - M. 1:1 mill. Norges Geologiske Undersøkelse.

Skilbrei, J.R. 1988. Flymagnetiske målinger over Barentshavet 1987. Norges geologiske undersøkelse. Internal NGU-report 88.156 (in Norwegian), 1-31.

Skilbrei, J.R. 1989a: Om bruken av "straight slope" metoden ved tolkning av dyp til magnetiske kilder; et empirisk studium med forslag til korreksjonsfaktorer til straight slope lengden. NGU-rapport 89.170 (in Norwegian), 1-18.

Skilbrei, J.R. 1989b: En test av autokorrelasjonsmetoden ved estimering av dyp til magnetisk grunnfjell (Mapran 3-programmet). NGU-rapport 89.171 (in prep.).

Skilbrei, J.R., Kihle, O., Christoffersen, T. & Myklebust, R. 1988: Spitsbergen Aeromagnetic Survey. Interpretation report. Confidential NGU-report 88.221, 1-42.

Skilbrei, J.R., Håbrekke, H., Christoffersen, T. & Myklebust, R. 1990: Aeromagnetic surveying at high latitudes, a case history from the northern Barents Sea. First Break, Vol. 8, No. 2, 46-50.

Skilbrei, J.R., Skyseth, T. & Olesen, O. 1990: Petrophysical data and opaque mineralogy of high grade and retrogressed lithologies: Implications for the interpretation of aeromagnetic anomalies in northern Vestranden, Western Gneiss Region, Central Norway. Tectonophysics (in press).

Spencer, A.M., Home, P.C. & Berglund, L.T. 1984: Tertiary structural development of the western Barents Shelf: Troms to Svalbard, In: Petroleum Geology of the North European Margin (Ed. A.M. Spencer), Graham and Trotman, London, 199-209.

Steel, R.L. & Worsley, D. 1984: Svalbard's post-Caledonian strata - an atlas of sedimentational patterns and palaegeographic evolution, In: Petroleum Geology of the North European Margin (Ed. A.M. Spencer), Graham and Trotman, London, 109-135.

Steel, R.J., Gjelberg, J., Nøttvedt, A., Helland-Hansen, W., Kleinspehn, K. & Rye-Larsen, M. 1985: The Tertiary strike-slip basins and orogenic belt of Spitsbergen. Soc. Econ. Paleont. Mineral Spec. Publ. 37, 339-359.

Steenland, N.C. 1963: Discussion on "An evaluation of basement determinations from airborne magnetometer data" by Peter Jacobsen, Jr. (Geophysics 24, 309-319), Geophysics 28, 491-492.

Steenland, N.C. 1970: Recent developments in aeromagnetic methods. Geoexploration, 8, 185-204.

Thorning, L. 1982: Processing and interpretation of aeromagnetic data in The Geological Survey of Greenland. Geol. Survey of Greenland. Report no. 114, 31-34.

Vacquier, V., Steenland, N.C., Henderson, R.G. & Ziets, I. 1951: Interpretation of aeromagnetic maps. Geol. Soc. Am. Mem., 47, 151pp.

Vacquier, V. 1972: Geomagnetism in Marine Geology, Elsevier, Amsterdam, New York.

Weigand, P. W. & Testa, S. M. 1982: Petrology and geochemistry of Mesozoic dolerites from the Hinlopstretet area, Svalbard. Polar Research, 1, 35-52.

Winsnes, T.S. & Worsley, D. 1981: Geological Map of Svalbard 1:500,000 Map Sheet 2G Edgeøya. Norsk Polarinstitutt Skrifter 154 B, 29-38.

Worsley, D. & Edwards, M.B. 1976: The Upper Palaeozoic succession of Bjørnøya, Norsk Polarinstitutt Årbok 1974, 17-34.

Åm, K. 1972: The arbitrarily magnetized dyke: interpretation by characteristics. Geoexploration, 10, 63-90.

Åm, K. 1975a. Magnetic profiling over Svalbard and surrounding shelf areas. Norsk Polarinstitutt Årbok 1973, 87-99.

Åm, K. 1975b: Aeromagnetic basement complex mapping north of latitude 62^0N, Norway. Nor. geol. unders. Bull. 316, 351-374.

LIST OF FIGURES

Fig. 1: Aeromagnetic survey area covering the northern Barents Sea. Flight lines used in the gridding process are shown. Inset in upper right corner shows location of the map area. Inset in upper left corner shows areas I,II and III which were flown in order of priority. Diagonal solid lines indicate area I; the dotted pattern indicates area II. Simplified Svalbard geology from Steel & Worsley (1984). In Svalbard, HH, LP, D, M, and T denote surface exposures of Hecla Hoek, Late Palaeozoic, Devonian, Mesozoic and Tertiary rocks, respectively. FG: Forlandsundet Graben. BF: Billefjorden Fault. LF: Lomfjorden Fault. CB: Central Graben Basin. Location of deep reflection line IKU-85-H is shown (eastern part of this line is outside survey area).

Fig. 2: Aeromagnetic residual map (simplified version) covering the northern Barents Sea. The International Geomagnetic Reference Field (IGRF) epoch 1985 has been subtracted. Contour interval is 20 nT. H and L denote magnetic high and magnetic low (hatched area), respectively.

Fig. 3: East-west profile (pr. no. BSA-7714-3-A) across Storfjorden showing high-frequency anomalies of weak amplitudes in an area which is an otherwise flat magnetic region (no anomalies originating from deep sources). To the left (west) on the profile is an anomaly with its source interpreted to lie at a depth of 4 km. To the east is an anomaly from north of Hopen (Hopen High).

Fig. 4: Colour map (shaded relief version with illumination from the east) of residual aeromagnetics. Contour interval is 10 nT.

Fig. 5: Depth to magnetic basement map. Contours show depth below sea level in km. Interpreted faults, continent-ocean boundary, and a major tectonic boundary are shown.

Fig. 6: Line drawing of deep reflection profile (unmigrated time section, line IKU-85-H) running NNW-SSE across the Svalbard Platform showing different crustal terranes. Location in Fig. 1. TP: Top Permian. A: Westward dipping reflection. B: Single contineous reflection. TWT: Two-way travel time. After Gudlaugsson et al. (1987).

Fig. A1: Thin magnetic sheet source with its magnetic response g(x). The source extends to infinity along $^{+}/_{-}$ y and +z. The top of the source is at the depth z_1 below the observation plane. After Phillips (1975).

Fig. A2: Interpretation principle of the autocorrelation method. (A) A shallow magnetic dyke causes a narrow anomaly. The correlation of the waveform with itself is consequently small. (b) A deep-seated dyke causes a long-wavelength anomaly with a higher degree of autocorrelation. The depth is calculated from estimated maximum entropy autocorrelation coefficients of the magnetic profile (one depth for each position). After Olesen et al. (1990).

Fig. A3: Schematic response of Phillips (1975) autocorrelation method to a block model of finite thickness having uniform magnetization. Top, magnetic anomaly; middle, the block model; bottom, the output of the estimated magnetic source depth. Crosses denote primary depth estimates (n=1), dots denote output at higher lags (n=2,3,4). After Kovacs & Vogt (1982)

Fig. A4: Schematic output of the autocorrelation depth to source method (Phillips 1975) for a three-dimensional source. Same convention as in Fig A3. After Kovacs & Vogt (1982)

Fig. 1

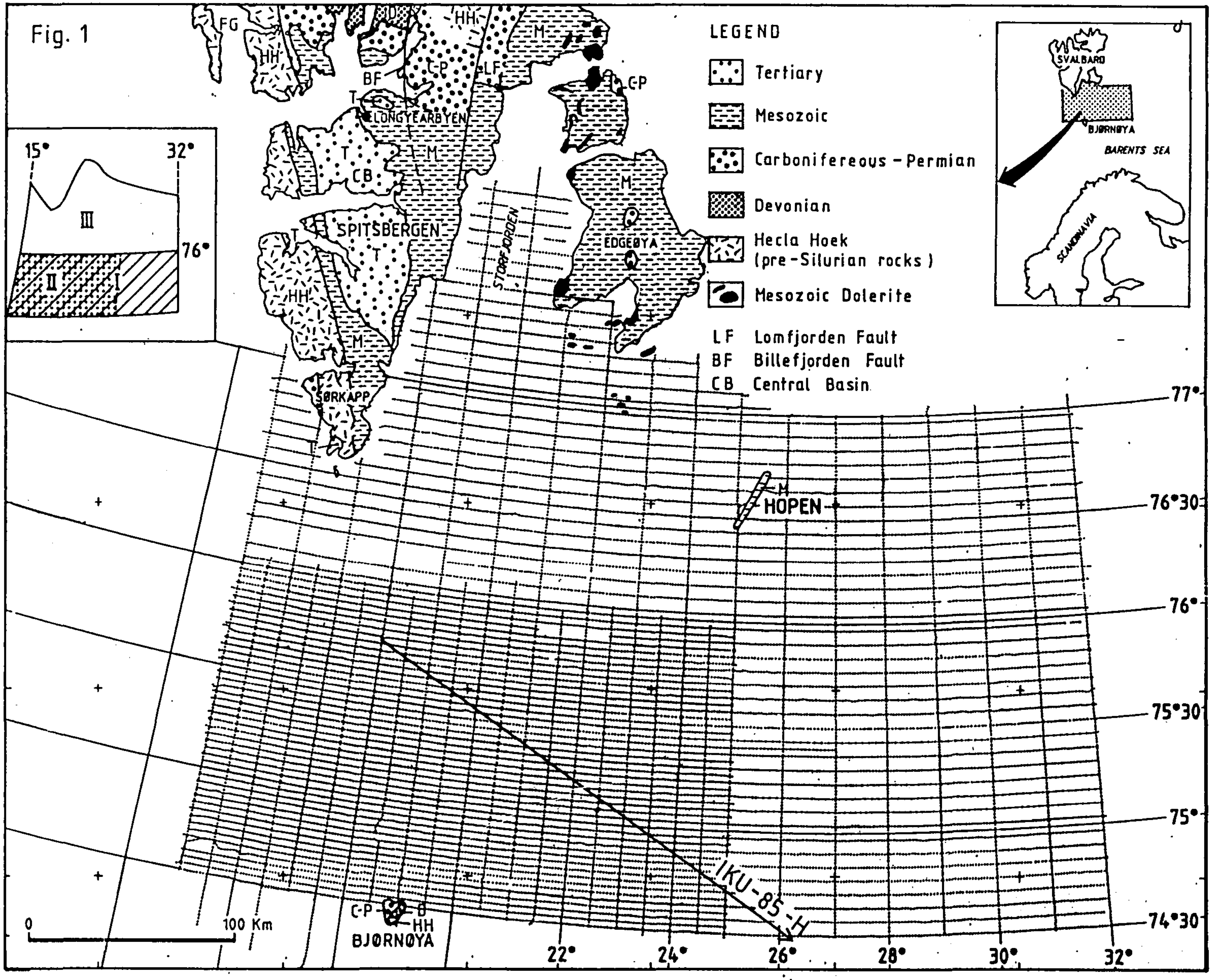
LEGEND
Tertiary
Mesozoic
Carboniferous - Permian
Devonian
Hecla Hoek
(pre-Silurian rocks)
Mesozoic Dolerite
LF Lomfjorden Fault
BF Billefjorden Fault
CB Central Basin
SPITSBERGEN
LONGYEARBYEN
STORFJORDEN
EDGEØYA
SØRKAPP
HOPEN
BJØRNØYA
IKU-85-H
SVALBARD
BARENTS SEA
SCANDINAVIA
0
100 Km
22°
24°
26°
28°
30°
32°
77°
76°30
76°
75°30
75°
74°30
15°
76°

Fig. 2

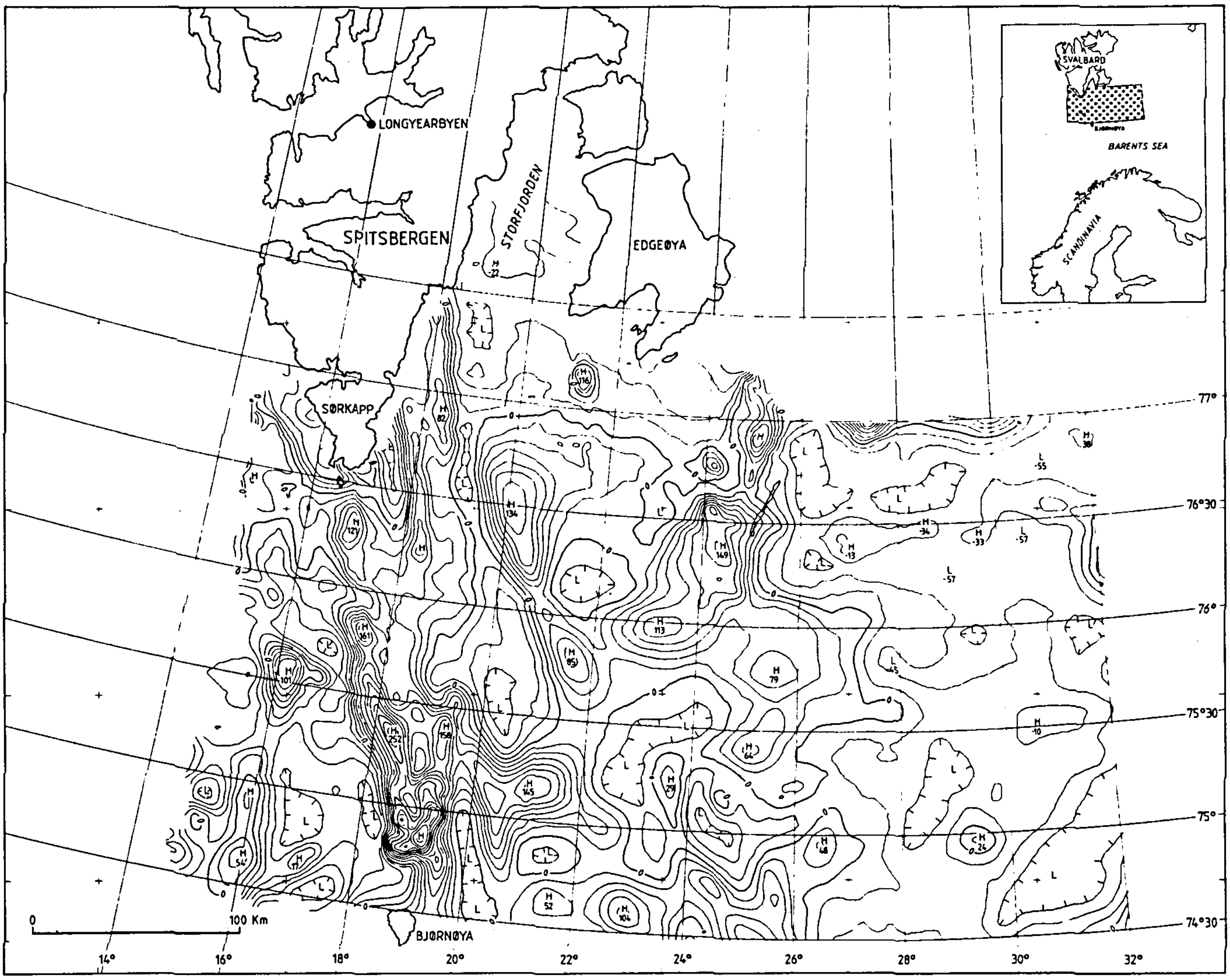
LONGYEARBYEN
SPITSBERGEN
STORFJORDEN
EDGEØYA
SØRKAPP
BJØRNØYA
SVALBARD
BARENTS SEA
SCANDINAVIA
0
100 Km
77°
76°30
76°
75°30
75°
74°30
14°
16°
18°
20°
22°
24°
26°
28°
30°
32°

Fig. 3

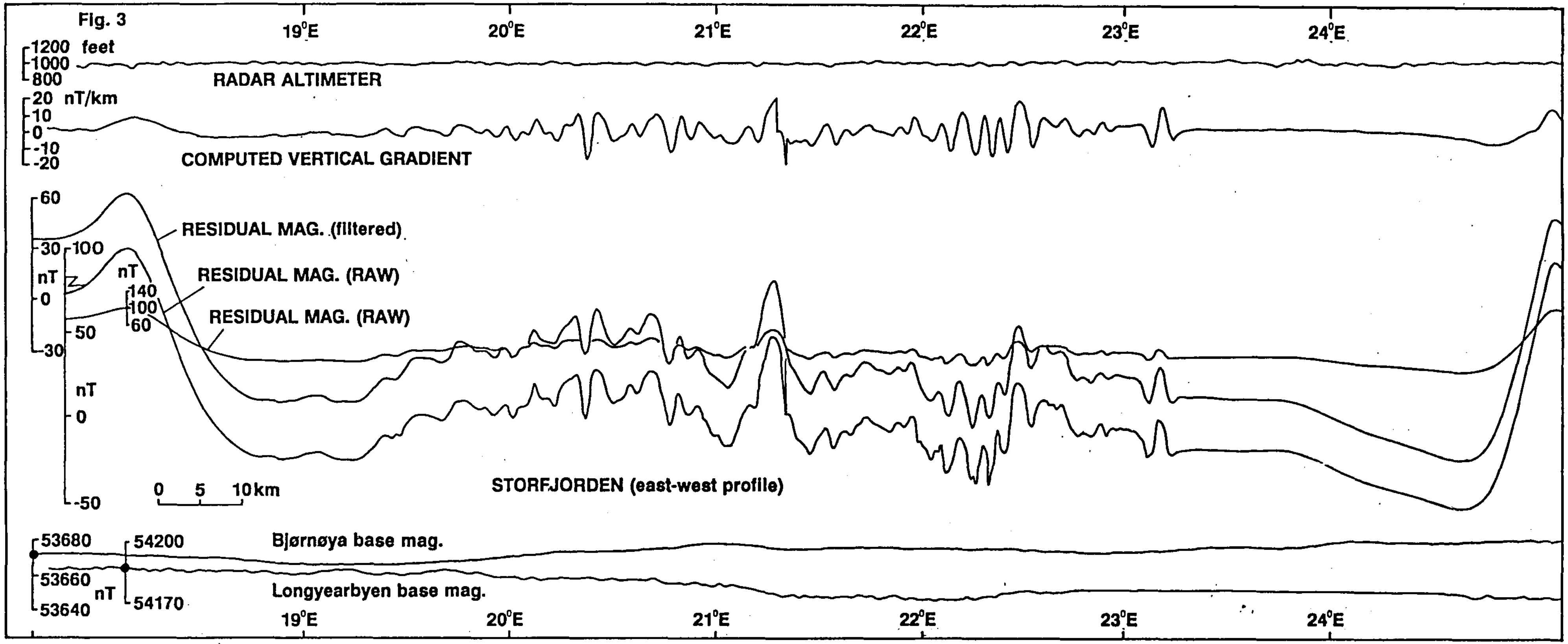

1200 feet
1000
800
RADAR ALTIMETER
20 nT/km
10
0
-10
-20
COMPUTED VERTICAL GRADIENT
60
30
nT
0
-30
RESIDUAL MAG. (filtered)
100
50
nT
0
-50
RESIDUAL MAG. (RAW)
nT
140
100
60
RESIDUAL MAG. (RAW)
0 5 10km
STORFJORDEN (east-west profile)
53680
53660
nT
53640
54200
54170
Bjørnøya base mag.
Longyearbyen base mag.
19°E
20°E
21°E
22°E
23°E
24°E

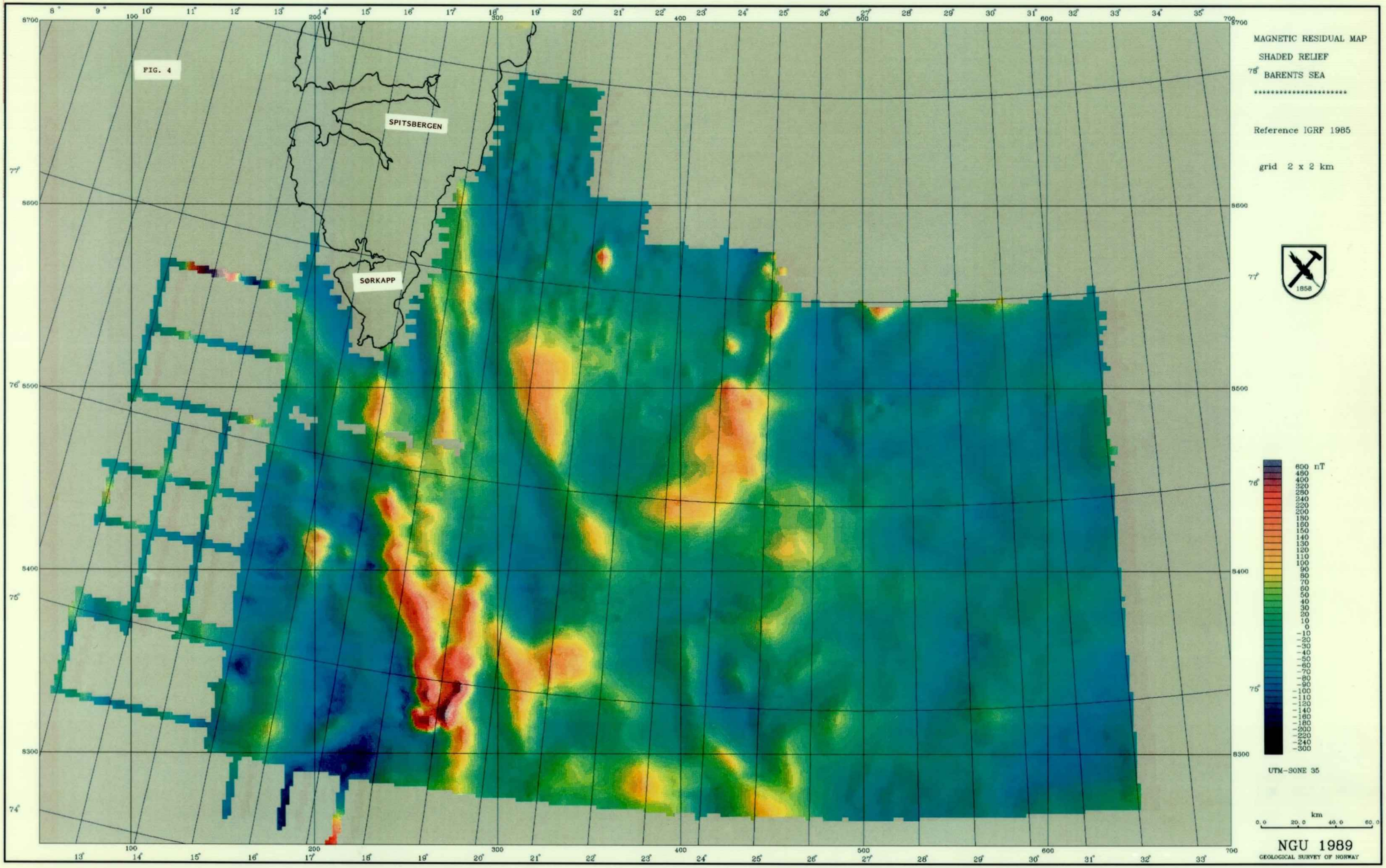
FIG. 4
SPITSBERGEN
SØRKAPP
MAGNETIC RESIDUAL MAP
SHADED RELIEF
BARENTS SEA
Reference IGRF 1985
grid 2 x 2 km
1858
600 nT
UTM-SONE 35
km
NGU 1989
GEOLOGICAL SURVEY OF NORWAY

Fig. 5

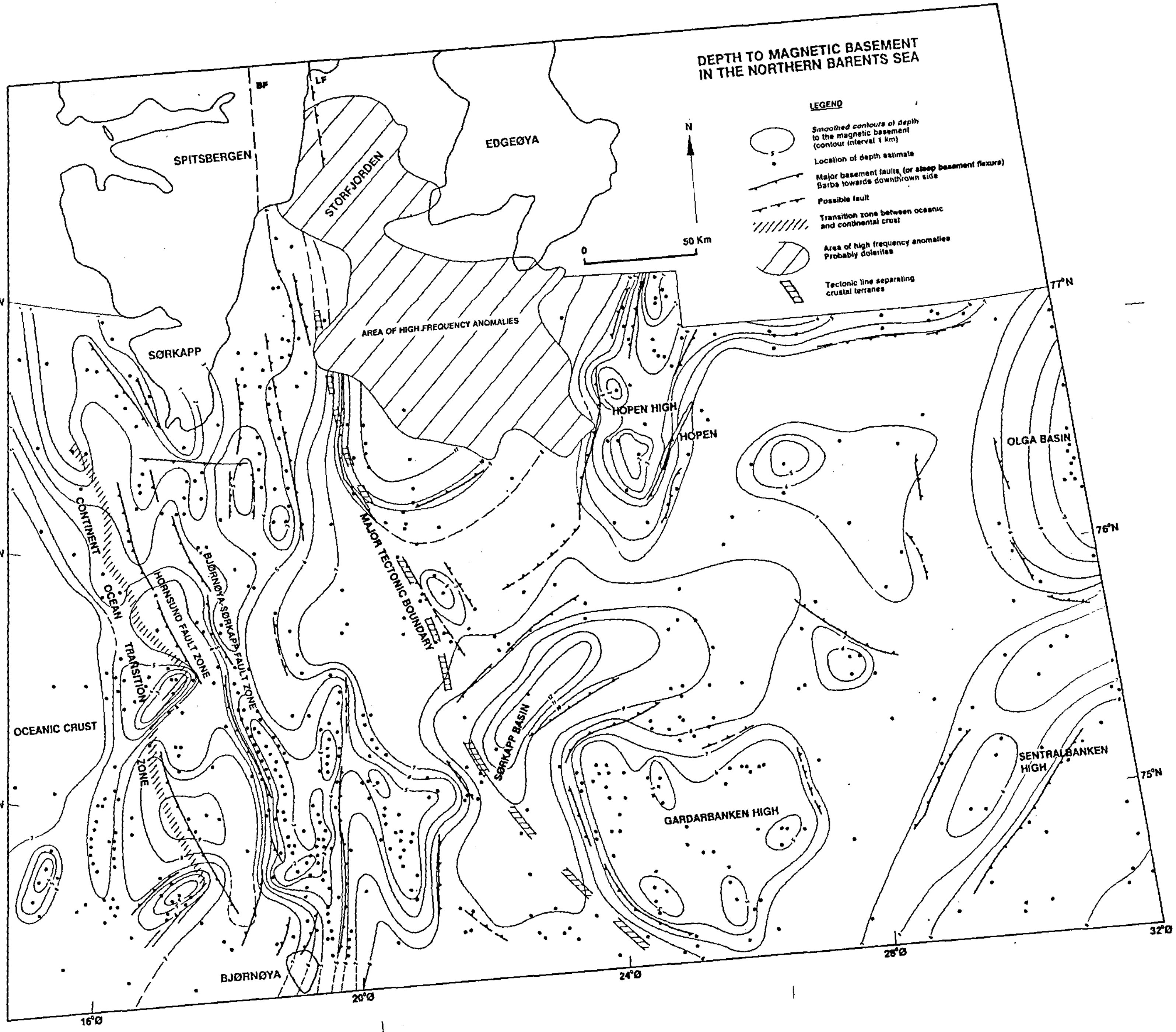

DEPTH TO MAGNETIC BASEMENT
IN THE NORTHERN BARENTS SEA
LEGEND
Smoothed contours of depth to the magnetic basement (contour interval 1 km)
Location of depth estimate
Major basement faults (or steep basement flexure) Barbs towards downthrown side
Possible fault
Transition zone between oceanic and continental crust
Area of high frequency anomalies Probably dolerites
Tectonic line separating crustal terranes
N
0
50 Km
SPITSBERGEN
BF
LF
STORFJORDEN
EDGEØYA
SØRKAPP
AREA OF HIGH FREQUENCY ANOMALIES
HOPEN HIGH
HOPEN
OLGA BASIN
MAJOR TECTONIC BOUNDARY
CONTINENT
OCEAN
TRANSITION
ZONE
HORNSUND FAULT ZONE
BJØRNØYA-SØRKAPP FAULT ZONE
OCEANIC CRUST
SØRKAPP BASIN
GARDARBANKEN HIGH
SENTRALBANKEN HIGH
BJØRNØYA
77°N
76°N
75°N
16°Ø
20°Ø
24°Ø
28°Ø
32°Ø

Fig. 6

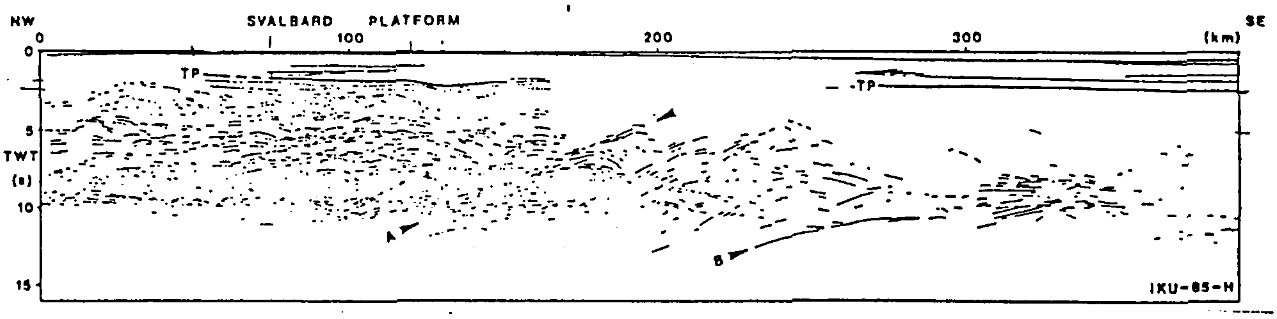
NW
SVALBARD PLATFORM
SE
0
100
200
300
(km)
0
5
TWT
(s)
10
15
TP
TP
A
B
IKU-85-H

APPENDIX 1

The autocorrelation method of Phillips (1975, 1978, 1979) was used to estimate the depth to magnetic basement automatically from the total field aeromagnetic profiles.

This brief description of the method follows, rather closely, the description given in Phillips (1979), Thorning (1982) and in Olesen et al. (1990). The magnetic basement is defined as a two-dimensional surface (Fig. A1) constructed from a large number of very thin vertical 'dykes'. The method assumes the following: 1. Each of the homogeneously magnetized dykes has vertical (and parallel) sides, horizontal tops which correspond to the top of the magnetic basement and extend to infinity in directions perpendicular to the profile (including vertically downwards). 2. The upper termination of the dykes is the basement surface. This depth can vary from dyke to dyke and thereby the dykes placed next to one another define the topography of the top of the magnetic basement. 3. Each dyke has a magnetization which may differ from that of the adjoining dyke. The depth is estimated by passing a short window along the magnetic profile, estimating a depth for each position of the window. It has to be assumed that the anomaly within such a given window originates entirely from sources at a certain depth.

The depth expressions are:

$$Z = \frac{n\Delta x}{2}\sqrt{\frac{1}{1/\phi_n - 1}} \qquad \left[Z = \frac{\Delta x}{2}\sqrt{\frac{2n+1}{\phi_n/\phi_{n+1} - 1} - n^2}\right]$$

where Δx is the sampling interval, n is the number of intervals in the autocorrelation lag and ϕ is the autocorrelation function.

The depth can be estimated from a value of the single autocorrelation at a single lag (1). According to Phillips (1975), the best depth estimate is always the depth curve calculated from the first lag (n=1), while higher lags (n=2,3,4) are used to check the validity of the estimate. A second solution (2) can be expressed in terms of the autocorrelation at two successive lags. Phillips (1975) also claims that sources at different depths can be separated using this formula, i.e., anomalies caused by deep and shallow bodies in the same profile. This will, of course, depend on there being sufficient separation between the anomalies showing different wavelengths. Although the method has been applied in depth determination (Thorning 1982, Vogt 1982, Olesen 1990), no rigorous study of the precision or the 'goodness' of the method has been published, to the author's knowledge. However, it is shown empirically (Skilbrei 1989) that the autocorrelation method yields basement depths that depend on the ratio of the width (w) of the dyke to the depth (d) to the top of the dyke (as the Peters, Sokolov and Straight-slope methods). This is perhaps intuitively to be expexted, since the form of a magnetic profile normal to the strike of a dyke which is homogeneously magnetized is dependent only on the ratio width/depth (w/d) and on the combined angle tetha (θ) (Åm 1972). It was also found that when the ratio w/d is between 2 and 4, and the assumptions that the method require are fulfilled, then the autocorrelation method yields depths which are near the true depths.

Fig. A2 illustrates the principles of the interpretation method. A shallow magnetic dyke causes a narrow anomaly. The correlation of the waveform with itself is consequently small. A deep-seated dyke causes a long-wavelength anomaly with a higher degree of autocorrelation.

As with other methods of determining source characteristics from potential field data, the depth-to-source algorithm used here gives its best results where the potential field is highly variable over short horizontal scales, that is, where the anomalous magnetic field is responding to relatively large contrasts in vector magnetization and/or depth of the basement rocks. In areas where these contrasts result in two-dimensional (linear) anomalies (Fig. A3), higher lags of the autocorrelation function formed by using multiples of the original window give depth estimates that are convergent or diverge only slightly downward with increasing lag number and window size. The best depth estimate, formed by the first autocorrelation lag using the original window, also tends to be slightly deeper than the actual depth to the source rocks. Both effects are due to differences between the semi-infinite dyke model used and the real sources, even in regions of purely two-dimensional anomalies lying perpendicular to the data track, and are typically a small fraction (<1/5) of the point spacing.

In areas having little or no magnetization and depth contrasts over the analysis window, the sources are said to be one-dimensional, that is, they are a function only of depth. When entering a magnetically featureless area, the algorithm tends to respond in much the same fashion as a seismic profiling system heading out over a large escarpment: the depth estimates trail downward more or less hyperbolically forming the equivalent of a side echo from the last good 'reflector' or source magnetization-depth contrast (Fig. A3). Higher lags of the autocorrelation, using larger windows, see this lack of a magnetic 'reflector' more quickly and the estimated values increase even more rapidly downward. Differences between source depth estimates in such areas can typically be an order of magnitude larger than errors in two-dimensional regions.

In regions of three-dimensional sources the seismic profiler analogy breaks down. Because the autocorrelation in such regions contains predominantly more high-frequency information (i.e., is 'spikier') than a two-dimensional source of the same depth, the estimated depth is shallower than the actual magnetic source depth (Fig. A4). Further, at higher lags the depth estimates will be even shallower due to the greater contamination of the autocorrelation by the high-frequency terms. Regions with three-dimensional sources therefore have negative depth estimate errors with higher lags, as opposed to one-and two-dimensional regions where the differences between estimates are positive with increasing lag number. In all cases, the first depth estimate at the primary autocorrelation lag is the best estimate regardless of the source structure.

The sign and magnitude of the differences between successive depth estimates can be interpreted to yield information about how well the local source morphology fits the algorithm's infinite dyke model, and provides a practical means of rejecting less valid depth estimates. In practice, a suitable combination of sampling interval and window length is chosen for each profile on the basis of available prior knowledge of the areas studied, and a trial run on the data line. The sampling interval and window length is then modified if anomalous depth estimate errors occurred: the window and sampling interval is broadened for regions showing predominantly one-dimensional behaviour initially, or shortened for regions showing predominantly three-dimensional behaviour.

FIG A1

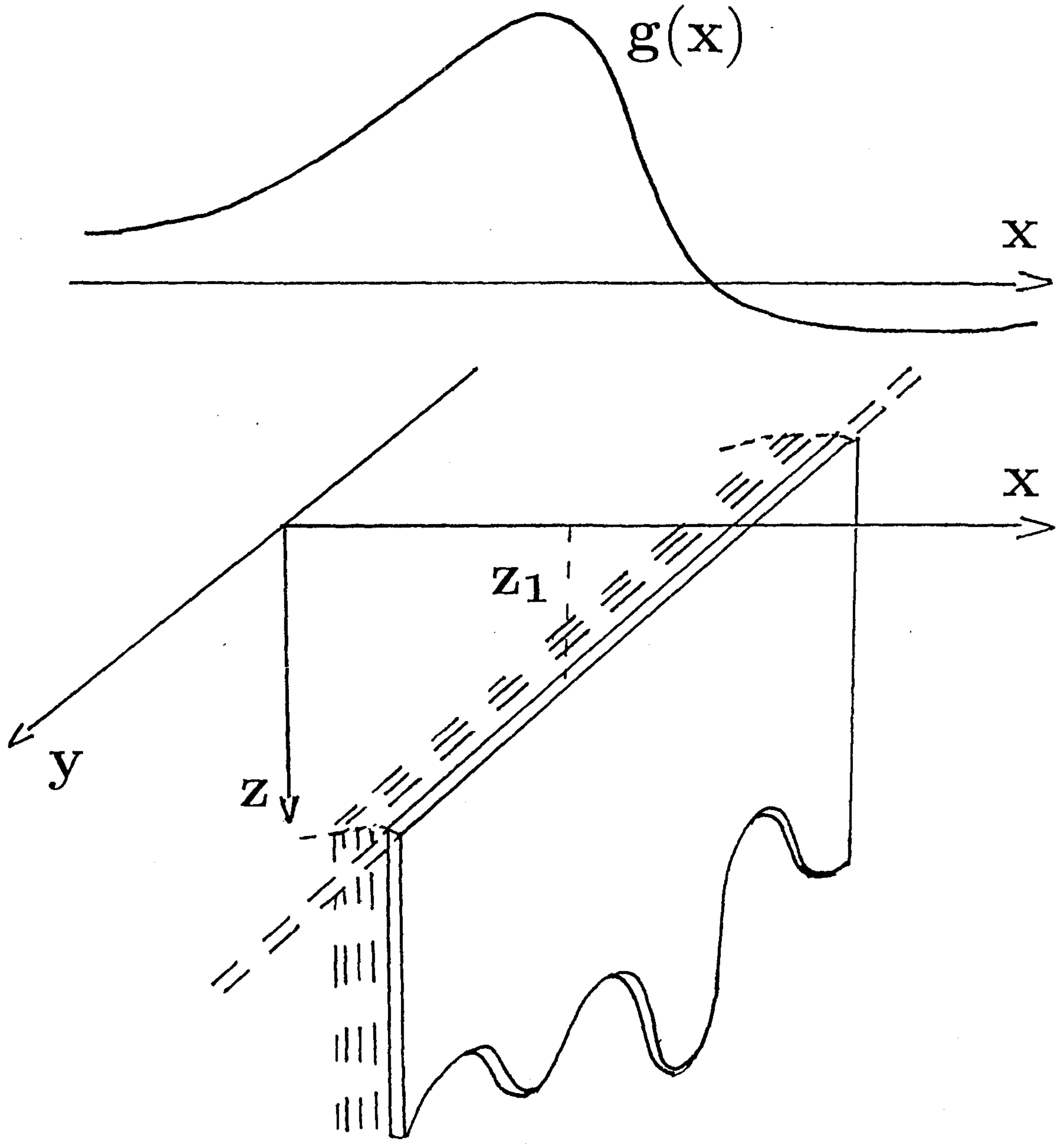

FIG A2

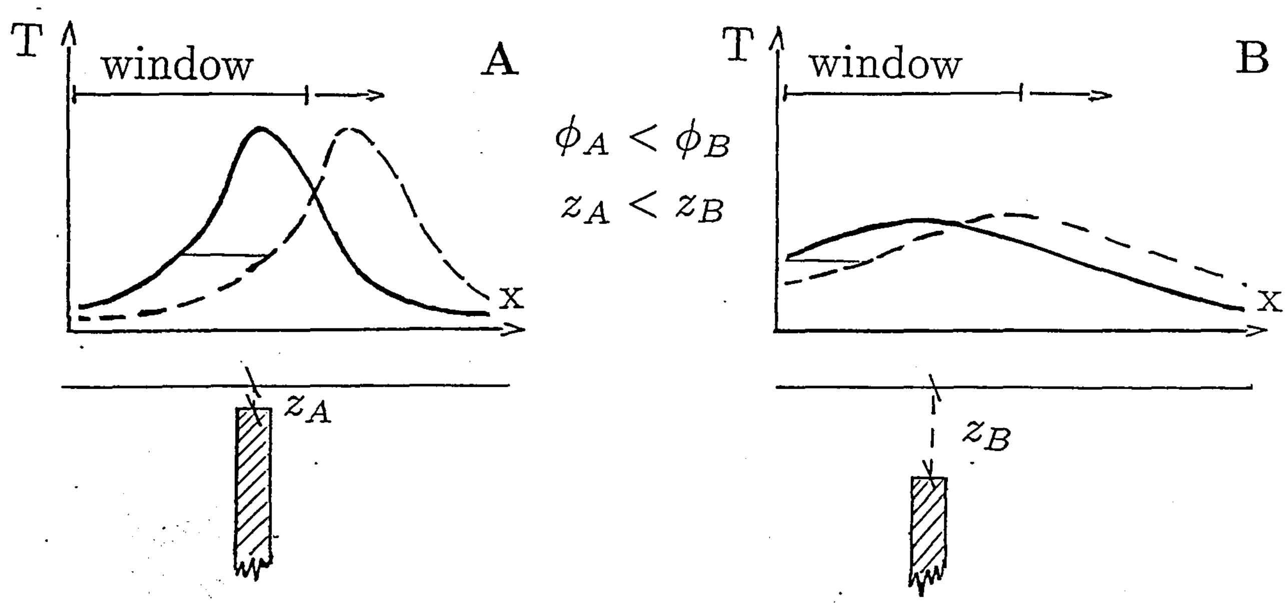

FIG. A3 TWO-DIMENSIONAL SOURCES

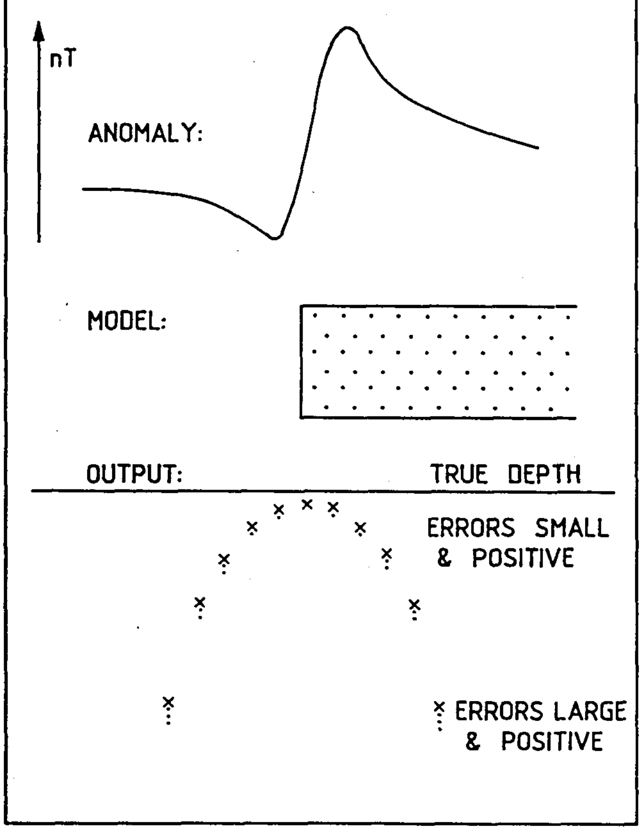

FIG. A4 THREE-DIMENSIONAL SOURCES

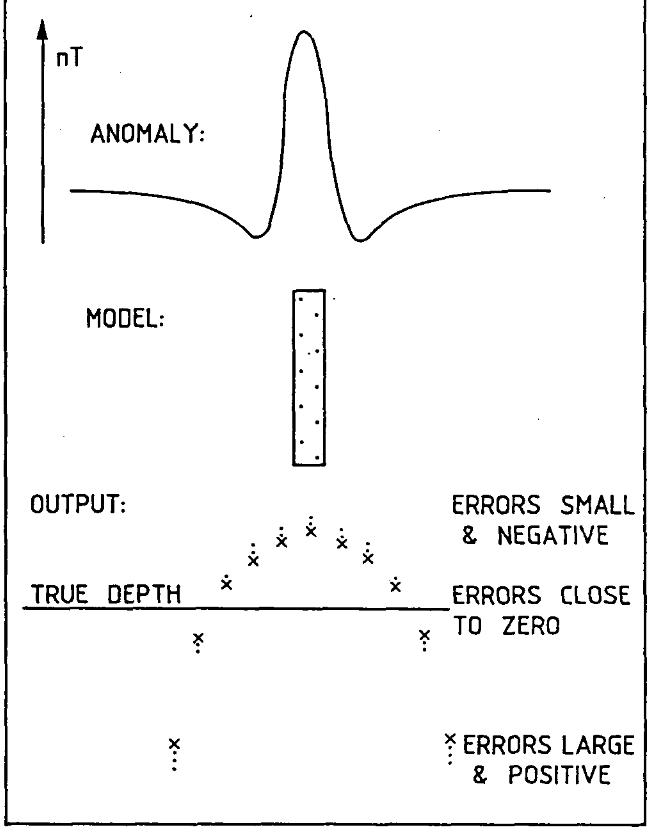


MAGNETIC RESIDUAL MAP
SHADED RELIEF
BARENTS SEA
****
Reference IGRF 1985
grid 2 x 2 km
1858
APPENDIX 2 NGU-REPORT 90.046
600 nT
480
400
320
280
240
220
200
180
160
140
120
110
100
90
80
70
60
50
40
30
20
10
0
-10
-20
-30
-40
-50
-60
-70
-80
-90
-100
-110
-120
-140
-160
-180
-200
-240
-280
-320
-360
-400
UTM-SONE 35
M 1 / 1 MILLION
km
0.0
20.0
40.0
60.0
NGU 1989
GEOLOGICAL SURVEY OF NORWAY

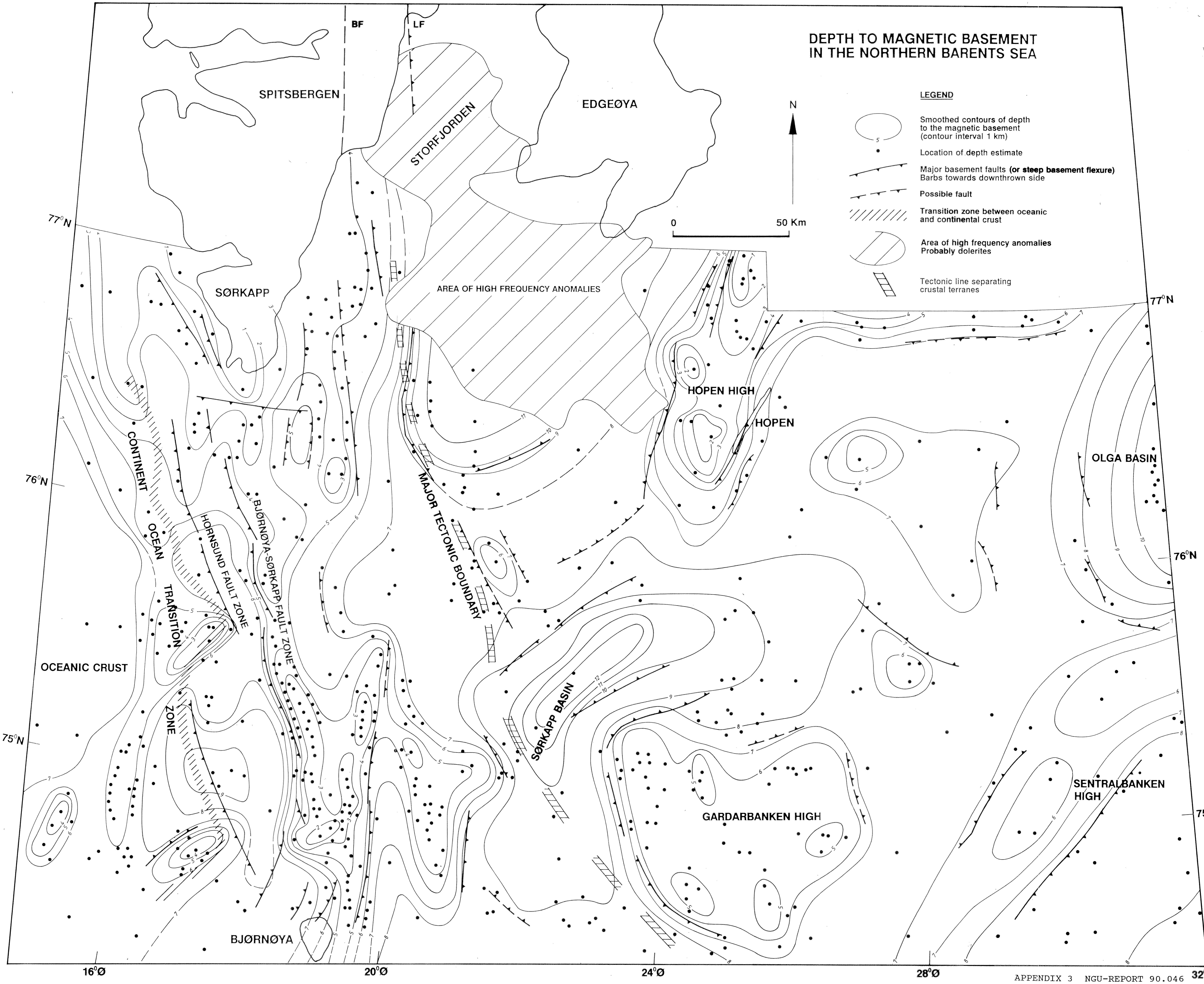

APPENDIX 3 NGU-REPORT 90.046